Theoretical Study of the Photophysics of Adenine in Solution: Tautomerism, Deactivation Mechanisms, and Comparison with the 2-Aminopurine Fluorescent Isomer

Benedetta Mennucci,*,† Alessandro Toniolo,‡ and Jacopo Tomasi†

Dipartimento di Chimica e Chimica Industriale, Università di Pisa, via Risorgimento 35, 56126 Pisa, Italy, and Dipartimento di Chimica Fisica ed Elettrochimica, Università di Milano, via Golgi 19, 20133 Milano, Italy

Received: December 31, 2000

The lower singlet excited states of isolated and solvated tautomers of adenine and of the fluorescent isomer 2-aminopurine have been studied with different quantum mechanical methods: geometries have been obtained at CIS level, while calculations of electronic structures have been performed using a multireference perturbed CI method and (for excitations) a TDDFT approach. In all calculations, the solvent (e.g., water) has been described within the IEF polarizable continuum model (IEF-PCM). The results have been successfully compared to experimental absorption and emission spectra. The same approach has been applied to the analysis of possible deactivation mechanisms acting on adenine but not on 2-aminopurine: both effects due to the proximity of $\pi \rightarrow \pi^*$ and $n \rightarrow \pi^*$ states and the chance of an intramolecular twisting of the amino group have been considered.

1. Introduction

Detailed knowledge and understanding of the electronic structure of the genetic material is one of the natural goals of science; in practice, this interpretation relies heavily on data for the excited-state properties of the constituent chromophores, the nucleic acid bases. A large number of theoretical and experimental studies have been performed (here we quote a "classic" review,[1] but many other more recent references will be given in the following); most spectroscopic studies refer to dilute aqueous solutions, whereas theoretical works, for the most part, have been focused on the gas phase. Calculations with explicit consideration of the solvent are in fact still limited, and in general, they have been based on simple solvent models (especially Onsager), and/or they have been focused on just few of all possible aspects of the problem. Consequently, the literature appearing so far on condensed-phase studies on DNA components mainly reduces to a set of fragmentary information with respect to the large and detailed body of gas-phase studies.

With this paper, we try to change this trend, aiming at realizing a coherent condensed-phase study more than a partial analysis of solvent effects. Both the nuclear and electronic structures of ground and excited states will be obtained in the framework of an accurate quantum mechanical solvation approach also including possible nonequilibrium phenomena between solute and solvent due to the dynamical nature of the problem.

In particular, the specific aspect we have selected within the huge field of possible investigations on DNA bases is the photophysics of adenine (6-aminopurine or Ade). Like the other nuclei acid bases (guanine, cytosine, thymine, and uracil), adenine is nonfluorescent at room temperature;[1] in other words, nature has developed a strategy to avoid damaging photochemistry in the nucleic acids carrying genetic materials. Such a strategy seems to be related to a mechanism that limits the excited state lifetime and thus lowers the resulting fluorescent quantum yield.

In the specific context of the adenine chromophore, it is interesting to introduce a comparison with its isomer 2-aminopurine (2AMP); it is in fact well-known that the fluorescence quantum yield for 2AMP in aqueous solution is 0.66[2] while it is only about 0.0003 for Ade,[1] and it is also known that their absorption spectra are rather different in the low-energy region. For all these reasons, 2AMP, which can be synthetically incorporated into DNA with little perturbation of the native double-helical structure, is often used as an intrinsic fluorescent probe in substitution of Ade.

Several possible deactivation mechanisms have been proposed to explain the low emission of Ade; here in particular, we recall the hypothesis of vibronic couplings between nearby excited states, which could cause the quenching of the luminescence, and the chance of conformational changes such as twisted intramolecular charge transfer, which could account for the differences in the photopysics of the two isomers. The objective of this work is to investigate the physical background for these very different absorption/emission properties of the two isomers when in the presence of a polar solvent like water.

Correlated quantum chemical calculations (DFT and CIS) will be used to investigate the geometry of ground and excited states and the spectroscopy (CI and TDDFT) of the two molecules in gas phase and in water solution; for the latter, the revised version of the polarizable continuum model (PCM),[3] which is known with the acronym IEF (integral equation formalism),[4] will be exploited.

2. Computational Details

Geometries. The geometry optimizations for ground and excited states both in vacuo and in water solution were performed with a development version of Gaussian program package.[5] The ground states were obtained at the density functional theory (DFT) using the hybrid functional which mixes the Lee, Yang, and Parr functional for the correlation part and

* Corresponding author. E-mail: bene@dcci.unipi.it.
† Università di Pisa.
‡ Università di Milano.

10.1021/jp0045843 CCC: $20.00
Published on Web 04/24/2001

the Becke's three-parameter functional for the exchange (B3LYP).[6] The basis set used was the correlation consistent valence double-ζ (cc-pVDZ) developed by Dunning.[7] To evaluate excited state geometries, we used the simple ab initio configuration interaction, including only single excited configurations (CIS). The basis set was still that used for ground-state DFT calculation. Also, for CIS optimizations and for the DFT ones, the solvent was analytically included both in the energy and the gradient step of calculation.[8,9]

Spectra and Transition Properties. To describe the ground and excited states of Ade and 2AMP, we used both the time-dependent density functional theory (TDDFT) and the multireference perturbation configuration interaction method, known with the CIPSI acronym,[10] with the same basis set exploited to get geometries.

Concerning the CIPSI algorithm, at each molecular geometry, both in solvent and in vacuo, configurations were selected with the "aimed selection" scheme;[11] this allows for defining a variational subspace of electronic configurations, giving a balanced description of all the electronic states of interest. The calculations in vacuo were made in two macroiterations (the first to get the natural orbitals used in the second one), which in turn are constituted by three perturbative selections (microiterations). For the calculations in solution, the macroiterations are repeated until convergency of the final variational energy for each electronic state (see below for further details). The resulting variational wave functions, expanded over up to about 16 000 selected determinants, were the basis for a diagrammatic quasidegenerate perturbation theory treatment,[10,12] with a Møller–Plesset (MP) partition of the Hamiltonian.

CIPSI calculations were carried out interfacing the original algorithm, modified as described in ref 13 so as to take into account the solvent, to a development version of GAMESS package.[14] The TDDFT calculations were run on a development version of Gaussian package.

Solvation. In the PCM-IEF solvation model,[4] the solvent is mimicked by a dielectric continuum with dielectric constant ϵ, surrounding a cavity with shape and dimension adjusted on the real geometric structure of the solute molecule. The latter polarizes the solvent and induces an electric field (the "reaction field") which interacts with the solute. In the IEF model, the solute–solvent electrostatic interaction is represented in terms of an apparent charge density spreading on the cavity surface, which gives rise to specific operators to be added to the Hamiltonian of the isolated system to obtain the final effective Hamiltonian and the related Schrödinger equation. Solvent terms depend on the solute wave function they contribute to modify, and thus, the problem requires the solution of a proper SCF scheme.

This is the general approach, in which solute electronic and nuclear charge distribution and solvent reaction field can mutually equilibrate; however, in vertical electronic transitions (both absorptions and emissions), the relaxation of the reaction field in the direction of the new solute electronic state may be incomplete. In particular, if we take into account the magnitude of the typical times characterizing electronic and nuclear (or molecular) motions, we can safely assume that in these fast phenomena only the part of the solvent reaction which is induced by the polarization of its electrons can immediately modify according to the new electronic state reached by the solute in the transition process, while all the rest remains frozen in the previous equilibrium condition determined by the initial state. In a reasonable approximation, the fast component can be taken proportional to the dielectric constant at infinite frequency ϵ_∞, where $\epsilon_\infty \approx n^2$ and n is the refractive index of the solvent. For water, the two values used for the dielectric constant are 78.39 and 1.776, for ϵ and ϵ_∞, respectively. In the framework of IEF-PCM, this scheme is realized introducing two sets of apparent charges representing the electronic (or fast) and the slow contributions of the solvent reaction, respectively.

As said before, the solute is embedded in a molecular cavity here obtained in terms of interlocking spheres centered on selected nuclei (the heavy atoms plus the hydrogens bonded to nitrogen). The chosen radii are 1.9 for the aromatic carbons bonded to an hydrogen atom, 1.7 for C bonded to amino nitrogen, 1.6 for all N, and 1.2 for hydrogens bonded to N. All the radii have been then multiplied by 1.2 in order to take into account the impenetrable core of the solvent molecules.[15]

We finally recall that in the PCM-IEF version used in this paper, to the solvent electrostatic reaction described above additional repulsive interactions between solute and solvent are included. For the latter, we have used the model originally formulated by Amovilli and Mennucci.[16]

TABLE 1: B3LYP/cc-pVDZ Geometrical Parameters of 9H and 7H Tautomers of Adenine in Vacuo and in Solution

	9H		7H		
	vac	water	vac	water	exp[a]
N1–C2	1.345	1.346	1.351	1.348	1.344
N1–C6	1.346	1.352	1.339	1.348	1.355
C2–N3	1.338	1.338	1.330	1.332	1.331
N3–C4	1.341	1.346	1.347	1.354	1.344
C4–C5	1.401	1.402	1.410	1.406	1.396
C5–C6	1.414	1.417	1.410	1.413	1.416
C5–N7	1.386	1.387	1.388	1.384	1.388
C6–N10	1.353	1.349	1.366	1.352	1.340
N7–C8	1.313	1.318	1.375	1.364	1.323
C8–N9	1.382	1.377	1.312	1.322	1.368
C4–N9	1.379	1.376	1.347	1.382	1.372
N1–C2–N3	129.2	129.1	129.1	129.1	128.8
C2–N3–C4	111.0	111.1	112.8	112.6	110.8
N3–C4–C5	127.0	126.7	123.4	123.6	127.3
C4–C5–C6	115.8	116.2	118.5	118.8	116.4
C5–C6–N10	122.1	122.6	124.5	124.3	124.3
C4–C5–N7	111.5	111.1	105.1	105.2	110.3
C5–C4–N9	104.4	104.7	110.4	110.4	105.9
C5–N7–C8	103.9	103.9	106.0	106.3	103.8
N7–C8–N9	113.5	113.4	114.0	113.8	113.8

[a] Crystalline 9-methyl adenina.[21]

3. Results and Discussions

It has been shown both theoretically and experimentally that Ade exists in two tautomeric forms (9H-Ade and 7H-Ade) in water solution, with the 9H tautomer as the major component (about 80%)[17] while in the gas phase the 9H tautomer largely dominates.[18] This dependence on solvent has been explained by the 7H tautomer having a substantially larger dipole moment than that of the 9H tautomer. Furthermore, it has been said that the major part of the emission of Ade comes from the 7H tautomer.[19] Concerning AMP, recent experimental results show that the 9H tautomer is the predominant form present (>97%) and that the 7H contribution to fluorescence is very small.[2]

Following such suggestions in this work, we have limited the tautomeric analysis to Ade, treating 2AMP as the single 9H tautomer.

3.1. Ground-State Geometries and Properties. The most important geometrical parameters of the ground state of the two Ade tautomers and of 2AMP are collected in Tables 1 and 2, where the numbers used to labels atoms are reported in the following scheme for each of the three molecules (the angle θ

TABLE 2: B3LYP/cc-pVDZ Geometrical Parameters of 2-Aminopurine in Vacuo and in Solution

	vac	water	exp[a]
N1−C2	1.361	1.365	1.355
N1−C6	1.333	1.335	1.324
C2−N3	1.350	1.353	1.345
N3−C4	1.330	1.331	1.319
C4−C5	1.413	1.414	1.386
C5−C6	1.398	1.396	1.408
C5−N7	1.391	1.393	1.386
C2−N10	1.362	1.358	1.352
N7−C8	1.308	1.313	1.320
C8−N9	1.390	1.384	1.363
C4−N9	1.375	1.372	1.373
N1−C2−N3	127.7	127.1	126.7
C2−N3−C4	111.9	112.4	112.3
N3−C4−C5	126.8	126.5	127.3
C4−C5−C6	115.0	115.3	115.2
N1−C2−N10	115.6	115.9	116.2
C4−C5−N7	110.9	110.7	112.2
C5−C4−N9	104.7	104.9	104.4
C5−N7−C8	104.1	104.0	102.6
N7−C8−N9	113.8	113.8	114.1

[a] Ref 22.

gives the orientation, in positive values, of the transition dipole moment vector, according to the De Voe−Tinoco convention[20]).

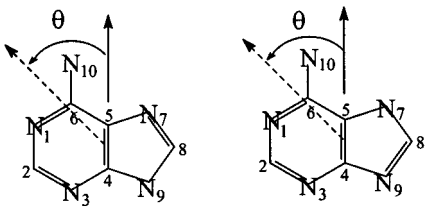

9H-Ade

7H-Ade

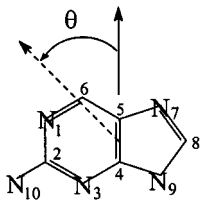

2AMP

All the geometries have been obtained without imposing any symmetry, but both in vacuo and in solution, the resulting structures are almost planar. The inclusion of solvent effects leads to small differences in the value of bond distances and bond angles in any of the three molecules. In general, the results agree with the available experimental data; however, such comparison lacks a real coherency, as both experimental references are not exactly the molecules we are studying—in particular for Ade, we report the neutron diffraction geometry of 9-methyladenine[21] and for 2AMP the X-ray structure of 9-[4-acetoxy-3-(acetoxymethyl)-butyl]-2-AMP.[22]

The agreement is sufficiently good also with previous calculations exploiting different approaches (we mainly refer to MP2 and CASSCF data);[24−26] for computations, the comparison is necessarily limited to gas-phase results, as no clear computed data are available for solvated structures (to the best of our knowledge). The only significant difference is in the out-of-plane angles of the amino hydrogens which, for both Ade and AMP, were computed to be about ±21° at the MP2/cc-pVDZ level (the improvement of the basis set showed no significant changes).[24,25] For a detailed discussion on the quality of ab initio structures for these and related molecules including comparisons with experiments, the interested reader is referred to ref 24.

TABLE 3: Dipole Moments (*D*) and Relative (free) Energy Difference (kcal/mol) between 9H and 7H Tautomers of Adenine in Vacuo and in Water Solution

	CIPSI		DFT		
	vac	water	vac	water	exp (dipole)
		9H			
μ	2.44	3.16	2.33	3.20	
		7H			2.4[a]−(3.0 ± 0.2)[b]
Δ	+6.92	+2.12	+9.02	+3.17	
μ	7.38	10.23	7.33	10.27	

[a] Crystalline 9-methyladenina.[27] [b] 9-Butyladenina in water.[20]

Contrary to what was found for geometries, both the dipole moment and the tautomerism between 9H and 7H forms of Ade are largely affected by the solvent.

As shown in Table 3, the dipole moments of both tautomers increase in water with respect to gas-phase by ∼1 D and ∼3 D on the 9H and 7H tautomers, respectively. Both CIPSI and DFT calculations show that the 9H tautomer is energetically favored both in vacuo and in water, where, however, the contribution of 7H increases due to its larger dipole moment (∼10 vs ∼3 D); the relative (free) energy difference between the two tautomers goes from 6.92 kcal/mol (9.02 at DFT level) to 2.12 kcal/mol (3.17 at DFT level), passing from gas phase to solution. These findings agree with both experimental[20,27] and previous theoretical data.[28]

3.2. Absorption. The analysis of the observed absorption spectrum of adenine is rather complicated due to two almost overlapping transitions in the first absorption band. Furthermore, this strong overlapping makes the evaluation of oscillatory strengths largely uncertain; in fact, to obtain oscillatory strengths for each individual transition, some type of band fitting is necessary, and in the case of adenine, this methodology is complicated by the fact that the two involved transitions are so close to overlap. Even more complex is the determination of the transition moment directions.

The "historical" information we have is that the UV/vis absorption spectrum of Ade exhibits a low-energy band, with a peak measured around 252 nm (4.9 eV) in the gas phase which is red-shifted to ∼260 nm (4.8 eV) in water solution.[29] Since the first observation by Stewart and Davidson in 1963,[30] it has been confirmed multiple times using various spectroscopic techniques that this band contains at least two electronic transitions. In water solution and crystal environments, the transitions are separated by approximately 10 nm, and typically, the first transition is weaker and centered around 270 nm (4.6 eV).[31] $n \rightarrow \pi^*$ transitions are also expected to be present in the electronic spectrum at intermediate energies. They are, however, about 2 orders of magnitude less intense than $\pi \rightarrow \pi^*$ transitions. Clark has tentatively assigned $n \rightarrow \pi^*$ transitions in adenine at 244 nm (5.08 eV) and around 204 nm,[32] but completely sure data are not available yet. Recent film dichroism and emission anisotropy studies of the purine and 2-aminopurine chromophores have enabled the identification of $n \rightarrow \pi^*$ transitions below (purine) and above (2-aminopurine) the lowest $\pi \rightarrow \pi^*$ transition.

Information concerning transition moment directions stems, on one hand, from polarized absorption spectra on 9-substituted adenine derivatives in the solid state[31,32] and, on the other hand, from linear dichroism measurements on 7 and 9 methyladenine

TABLE 4: Summary of Experimental and Present Theoretical Values (CIPSI and TDDFT) for the Excitation Energies (eV) for Adenine Tautomers in Vacuo and in Water[a]

	CIPSI		TDDFT		
	vac	water	vac	water	exp[b]
			9H		
$n\pi^*$	4.96	5.03	4.97	5.11	
f	0.001	0.00	0.000	0.000	
$\pi\pi^*$	4.97	4.61	5.08	5.02	4.55
f	0.010	0.097	0.167	0.219	0.05/0.09[c]
θ	−47	+77			+66[d]/+83[c]
$\pi\pi^*$	5.34	4.98	5.35	5.29	4.81
f	0.359	0.164	0.065	0.085	0.18[c]/0.24
θ	+53	+45			+19[d]/+35[c]
			7H		
$n\pi^*$	4.85		4.80	5.12	
f	0.071		0.001	0.001	
$\pi\pi^*$	4.89	4.64	4.97	4.97	4.53
f	0.076	0.143	0.0934	0.152	0.11
θ	+14	+21			+45[d]
$\pi\pi^*$	5.56	5.00	5.36	5.35	4.90
f	0.037	0.066	0.002	0.050	0.09
θ	+15	−2			−16[d]

[a] Experimental data refer to 9 and 7 methyl adenine (9 and 7 MA). [b] In water solution.[23] [c] In crystals.[31,32] [d] In PVA film with an error of ±7°.[23]

partially aligned in stretched PVA film.[23] For the first two transitions, resulting transition moment directions are very similar in the two studies. Thus, both crystal measurements and stretched film measurements indicate that the lowest $\pi \rightarrow \pi^*$ transition is polarized at an angle θ (see the scheme above for the definition) of about +83° to +66° from the short molecular axis and that the second transition is polarized at an angle of about +19° to +35°, depending on the surrounding environment. However, the oscillatory strengths of both transitions show significant variations between the two sets of experiments. The oscillatory strength determined in PVA film for the lowest transition is only 0.05, whereas that estimated for crystal is 0.09. For the second transition, PVA estimate of the oscillatory strength is 0.24 and crystal one is 0.18. It can, however, be noted that the sum of the oscillatory strengths for the lowest $\pi \rightarrow \pi^*$ transitions are almost the same regardless of methodology.

Passing to calculations, in Table 4, we report the CIPSI and TDDFT results of the three lowest transitions for the two tautomers of Ade both in vacuo and in solution. We recall that in these and in all the following calculations, the zero-point energy (ZPE) variations passing from one electronic state to a different one have been neglected.

As the 9H tautomer has been experimentally established (and confirmed by our calculations) as the predominant form both in the gas phase and in solution, we will try to interpret the Ade spectrum preferentially considering the 9H transitions, adding results obtained for 7H as corrections (especially for water solution, where the higher polarity of 7H-Ade stabilizes this tautomer with respect to the 9H form).

As a first point of discussion, let us consider a theoretical aspect, namely, the comparison between the two different levels of calculation. We can note that CIPSI and TDDFT results are very similar for gas phase (the being difference always less than 0.1 eV, with the exception of the second $\pi \rightarrow \pi^*$ transition in 7H Ade, for which the difference is around 0.2 eV). Significantly larger differences, on the contrary, can be found for solvated systems for which CIPSI always gives lower absorption energies than TDDFT of about 0.2−0.4 eV. This discrepancy between the two methods can be explained taking into account the different characteristics of the two approaches when applied to solvated systems.

We note that both methods consider possible solvent nonequilibrium effects due to the fast transition process, during which the slow component of the solvent response remains fixed to the value obtained after equilibration with the initial, ground state; thus, the main reason for their discrepancy has to be searched elsewhere, for example, in the basic structures of the two calculations. In the TDDFT approach, as in a random phase approximation (RPA) scheme for the Hartree−Fock wave function, excitation energies are obtained directly from the HF ground state. On the contrary, in the CIPSI calculation, a real CI construction of each state is computed; this requires some specific refinements when coupled to the solvation IEF model.

In particular, to take into account the dependency of the solvent response on the solute wave function, we nested an additional iterative procedure (indicated as macroiteration) to the general CI algorithm. This algorithm, with the following CI-diagonalization and evaluation of the density matrix, is repeated so that at each step m, a new set of apparent charges computed from the density matrix of step $m - 1$ is calculated and used to evaluate the current solvent operators. The procedure is repeated until convergency on the final energy is obtained (such a scheme constitutes the macroiteration). In addition, the molecular orbitals defining the CI basis are renewed at each step of the macroiteration in terms of the current natural orbitals; in this way, in fact, solute wave function and solvent charges can completely readjust in a self-consistent scheme. The complete application of this scheme means that each electronic state (ground and excited) requires a separated calculation involving a macroiteration optimized on the specific state of interest. This procedure is then generalized to include nonequilibrium effects by performing first a ground-state calculation from which the slow apparent charges and the related energies are obtained and saved in a file, and then a successive calculation on the excited state with the previous ground-state apparent charges as an additional source of solvent reaction.

If we go back now to the original question (possible reasons for CIPSI-TDDFT differences in solution), keeping in mind this scheme for the construction of the different electronic states in solution, we can understand why CIPSI excited states which are computed with a more complete coupling between solute and solvent can be stabilized more than in a TDDFT approach and thus why the resulting CIPSI absorption energies are always lower.

Passing to chemical aspects involving comparisons with the experimental evidence, data reported in Table 4 show that for the gas phase, CIPSI and TDDFT results are very close and they both sufficiently agree with the only measured data available in the literature for the vapor (i.e., a band around 4.9 eV).[29] For the comparison with previous calculations, we mainly refer to the CASPT2 results obtained by Fülscher et al.:[33] the main difference between this study and our present results is the relative position of the $n \rightarrow \pi^*$ state (which is the lowest one at the CIPSI level for both tautomers while is the third at CASPT2 for 9H Ade), while $\pi \rightarrow \pi^*$ transition energies sufficiently agree.

For solution, CIPSI behaves much better than TDDFT. The larger stabilization of the excited states obtained within CIPSI scheme in fact allows to obtain absorption energies very close to the experiments (4.61 and 4.98 eV computed for 9H Ade with respect to 4.55−4.81 eV[23]). This behavior does not significantly change if we also consider the other possible isomer (7H), as both its absorptions differ of less than 0.05 eV with

TABLE 5: Summary of Experimental and Present Theoretical Values (CIPSI and TDDFT) for the Excitation Energies (eV) of 2-Aminopurine in Vacuo and in Water[a]

	CIPSI		TDDFT		
	vac	water	vac	water	exp[a]
$\pi\pi^*$	4.26	4.07	4.40	4.27	4.05
f	0.212	0.171	0.126	0.147	0.10
θ	+78	+72			+50
$n\pi$	4.46	4.51	4.47	4.52	~4.5
f	0.004	0.002	0.002	0.002	
$\pi\pi^*$	5.58	5.22	5.48	5.45	5.13
f	0.208	0.103	0.045	0.039	0.06
θ	−64	−72			−70

[a] In water solution.[2]

respect to those of 9H Ade; the experimental data for 7MA confirm this similarity.[23]

Concerning the $n \rightarrow \pi^*$ transition, the most evident result is that in gas phase (both at CIPSI and TDDFT level), it is the lowest one with transition energy very close to the first $\pi \rightarrow \pi^*$ transition, while in solution, it is shifted to the second (TDDFT) and the third (CIPSI) position. Unfortunately, this shift cannot be confirmed by experimental data (due to the small probability for this transition); however, the low dipolar character of the corresponding excited electronic state gives a sufficient proof about the accuracy of our results, indicating a clear destabilization of the $n \rightarrow \pi^*$ state with respect to the more polar $\pi \rightarrow \pi^*$ states in water solution. More details on this point will be given below in the analysis of possible de-excitation processes.

The good agreement of the CIPSI solvated results with experiments is confirmed also by the analysis of both oscillatory strengths and transition moment directions (see the scheme above for the definition of convention). Concerning transition moment directions, much attention has been devoted to it from the experimental point of view even if the situation is still not completely clear. As reported above, the most recent results by Holmen et al. on PVA films of 7 and 9 MA[23] confirm what was previously determined by Clark for crystalline samples,[31,32] i.e., polarizations at angles of about +66°/+83° for the lowest $\pi \rightarrow \pi^*$ transition and +19°/+35° for the second one in 9MA. The computed values of θ in gas phase and in water solution are reported in Table 4 for both tautomers. The very good agreement of solvated results with both experimental data in the two different environments (the polymer matrix and the crystal) is evident.

Passing to 2AMP, the experimental absorption spectrum shows three major bands in the near-UV region, which have been assigned to the lowest $\pi \rightarrow \pi^*$ transitions, and a hidden weak low-lying $n \rightarrow \pi^*$ transition between the lowest two large bands. The related transition energies and properties are reported in Table 5 with the computed results obtained in vacuo and in water solution.

In the case of 2AMP, gas phase results also present some discrepancies between the two methods (CIPSI and TDDFT), especially for the lowest $\pi \rightarrow \pi^*$ transition (4.26 eV vs 4.40 eV). No experimental spectra exist for vapor-phase 2AMP or its derivatives, so calculated transition energies can be only validated by comparison with other calculations. The most accurate calculations have been recently done by Rachofsky et al.[34] at the CASSCF level, supplemented by multiconfigurational quasidegenerate perturbation theory (MCQDPT): in this case, the order of the excited states coincides with the present CIPSI calculation, and also, the excitation energies are in sufficient accord.

TABLE 6: Selection of Geometrical Parameters for the Lowest Singlet Excited States of 9H and 7H Adenine as Predicted with CIS/cc-pVDZ in Vacuo and in Water

	9H-Ade					7H-Ade	
	vac		water			vac	water
	HL	nπ^*	HL	HL1	$n\pi^*$	$\pi\pi^*$	$\pi\pi^*$
N1−C2	1.328	1.359	1.314	1.357	1.361	1.322	1.306
N1−C6	1.310	1.285	1.323	1.374	1.289	1.371	1.391
C2−N3	1.403	1.389	1.411	1.346	1.393	1.346	1.353
N3−C4	1.281	1.317	1.283	1.309	1.321	1.323	1.328
C4−C5	1.429	1.383	1.433	1.451	1.384	1.460	1.455
C5−C6	1.462	1.444	1.464	1.409	1.444	1.399	1.406
C5−N7	1.322	1.370	1.313	1.356	1.374	1.345	1.332
C6−N10	1.343	1.354	1.341	1.324	1.349	1.348	1.339
N7−C8	1.337	1.280	1.352	1.320	1.284	1.429	1.422
C8−N9	1.368	1.387	1.362	1.335	1.380	1.293	1.300
C4−N9	1.387	1.357	1.376	1.396	1.354	1.347	1.348
N1−C2−N3	127.0	114.0	127.0	129.6	113.9	130.7	130.9
C2−N3−C4	112.6	120.6	112.5	114.1	120.4	114.6	114.1
N3−C4−C5	126.8	124.6	126.8	124.0	124.6	120.8	121.5
C4−C5−C6	114.8	114.6	115.1	116.4	115.0	118.8	118.8
C5−C6−N10	118.9	120.4	119.9	122.8	121.0	125.2	125.4
C4−C5−N7	112.4	111.1	112.0	110.0	110.7	104.5	104.8
C5−C4−N9	103.0	104.7	103.3	103.5	104.9	109.8	109.6
C5−N7−C8	105.2	105.1	105.4	104.7	104.9	106.8	107.3
N7−C8−N9	112.4	112.5	111.6	115.3	112.7	111.8	113.4

Passing to solution, for which experimental data are well-known, we remark that CIPSI results present a good agreement with experiments both in the transition energies and in the transition properties (oscillatory strengths and transition dipole directions), while TDDFT transition energies are slightly too large. The considerations about differences between the two methods made for the parallel Table 4 of Ade could be repeated here. For 2AMP, an experimental value is available also for the low $n \rightarrow \pi^*$ absorption, and the corresponding computed value maintains the agreement observed for the other two bands both in the relative position of this absorption (between the two lowest $\pi \rightarrow \pi^*$) and in the absolute value of the transition energy.

3.3. Excited-State Geometries. The band maximum of fluorescence spectrum corresponds to an adiabatic (vertical) transition from the geometrically relaxed excited-state to the ground-state potential energy surface at a nonequilibrium position. Thus, the transition energy for the fluorescence has to be computed using the geometrically relaxed excited states. As said above, these geometries are obtained at the CIS level. We note that for solvated systems we assume a complete equilibration of all components of the solvent response to the electronic state we are considering in the geometry search; a qualitative valuation of the validity of this approach can be derived from simple considerations on specific solvent and solute relaxation times. As for the ground-state absorption, here we also consider two isomers for Ade and just one for 2AMP.

There is no experimental method to directly determine the excited-state geometries of molecules of this size, and thus, in Tables 6 and 7, we report the set of computed geometrical parameters for the singlet $\pi \rightarrow \pi^*$ and $n \rightarrow \pi^*$ states of Ade and 2AMP without making comparisons with experimental data.

For the 9H tautomer of Ade, the absorption results showed that between the two $\pi \rightarrow \pi^*$ absorptions, the lowest one is that with the smallest oscillator strength; this seems to suggest that both states (the lowest and the most probable) could contribute to the emission. This should not happen for both the 7H isomer and 2AMP, for which the lowest $\pi \rightarrow \pi^*$ transition coincides with that of larger probability (i.e., larger oscillatory strength): for both, we can thus explain the fluorescence

TABLE 7: Selection of Geometrical Parameters for the First Singlet $\pi \rightarrow \pi^*$ Excited State of 2-Aminopurine (2AMP) as Predicted with CIS/cc-pVDZ in Vacuo and in Water

	vac	water
N1−C2	1.325	1.325
N1−C6	1.348	1.349
C2−N3	1.387	1.393
N3−C4	1.311	1.307
C4−C5	1.430	1.435
C5−C6	1.430	1.433
C5−N7	1.345	1.336
C2−N10	1.332	1.327
N7−C8	1.319	1.336
C8−N9	1.356	1.348
C4−N9	1.367	1.363
N1−C2−N3	130.1	129.2
C2−N3−C4	109.4	110.4
N3−C4−C5	127.5	127.0
C4−C5−C6	116.8	116.6
N1−C2−N10	116.9	117.7
C4−C5−N7	110.1	110.1
C5−C4−N9	104.2	104.3
C5−N7−C8	105.5	105.6
N7−C8−N9	112.9	112.4

spectrum in terms of a single excited state. For these reasons, the geometry optimization in water solution has been repeated twice for the two different $\pi \rightarrow \pi^*$ states; for simplicity, let us indicate them according to the molecular orbitals which are mainly involved—we thus have HL (as the two MOs are HOMO and LUMO orbitals) and HL1 (as in this case the transition HOMO → LUMO+1 is the main one), respectively. The geometry of the HL1 state in vacuo is not reported, as the corresponding CIS optimization had serious convergence problems since the character of the state changed during the optimization.

Once again, the resulting structures are almost planar for all molecules (deviations of the dihedral angles from planarity are less than 1°); these findings are confirmed by previous papers using different quantum levels[26] and/or different basis sets.[25]

As observed for the ground states, here the geometries of the excited states also do not change too much passing from gas phase to solution. On the contrary, differences between ground and excited states are significant, especially in the aromatic part, with the 9H Ade state presenting the largest changes. These difference parallel the changes in electron density upon each excitation, as can be easily visualized in terms of the molecular orbitals mainly involved in the transition: for the two $\pi \rightarrow \pi^*$ transitions of 9H Ade in solution, these are reported in Figure 1.

Thus, in the HL state, the C2−N3 and C5−C6 bond distances are increased, and the adjacent N3−C4 and C5−N7 bonds are correspondingly shortened, consistently with the nodes of the LUMO, an antibonding orbital centered on C2 and C5. In parallel, the HL1 state shows the largest changes in the C4−C5 and C9−C8 bonds: the first is increased due to the presence of a node along the C4−C5 bond in the LUMO+1 antibonding orbital which is occupied, while the latter is shortened as this time the node appears in the HOMO but not in the LUMO+1.

Similar considerations can be also exploited to rationalize the differences in the geometry of the $n \rightarrow \pi^*$ excited state of 9H Ade and of the $\pi \rightarrow \pi^*$ of 7H Ade and 2AMP with respect to the corresponding ground states.

3.4. Fluorescence. As reported in the Introduction, the fluorescence quantum yield of Ade is very low; however, some experimental data are known, at least for the solvated molecule.[1]

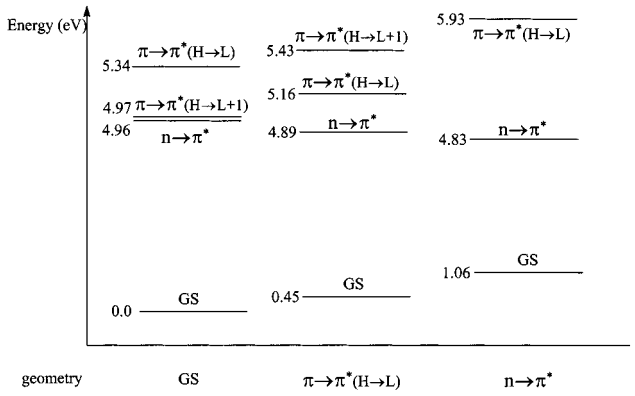

Figure 1. Gas-phase energy level diagram for 9H Ade: all energies (in eV) are with respect to the ground state (GS) energy at its optimized geometry.

TABLE 8: Summary of Experimental and Present Theoretical Values (CIPSI) of Fluorescence Energies (eV) for Adenine and Aminopurine in Vacuo and in Water

	vac		water		
	Ade				
	9H	7H	9H	7H	exp
$n\pi^*$	3.77		3.57		
$\pi\pi^*$(HL)	4.71	4.41	4.18	4.14	3.99[a]
$\pi\pi^*$(HL1)			3.99		
	2AMP				
$\pi\pi^*$	3.95		3.55		3.45[b]
$n\pi^*$	4.99		5.00		

[a] In water solution.[1] [b] In water solution.[26]

On the contrary, 2AMP has high fluorescent quantum yield, and experimental data are available in various solvents.

In Table 8, we report the experimental and calculated fluorescence energies of the two tautomers of Ade and of 2AMP. The two experimetnal values refer to water solution. All the results have been computed at CIPSI level, exploiting the CIS geometries optimized for each excited state in vacuo and in solution. For solution, the nonequilibrium scheme described in section 2 has been adopted with a solvent completely equilibrated with the emitting excited state, but only partially relaxed in the final vertical state that this time is represented by the ground state.

The first comment to make regards the effect of tautomerism on emission spectra of Ade. As said before, it was experimentally hinted that part of the emission of Ade arises from the 7H tautomer, and our results indicate that both in vacuo and in solvent the 7H contribution induces a decreasing of the emission energy and that in solution this goes in the correct direction for a better agreement with the experiment. However, for 9H tautomer, we have to take into account also the effect of the second $\pi \rightarrow \pi^*$ excited state we have commented above. The calculation of the emission energy for such a state in water solution (at its optimized geometry) leads exactly to the experimental result. This perfect equivalence can be fortuitous, due to some cancellation of errors; however, the shift toward lower emission frequencies, obtained by considering this additional excited state, can be a signal of a real contribution in the observed spectrum. As explained above, the contribution of this additional excited state can be safely neglected for both the 7H tautomer and 2AMP; for both molecules in fact, the excited state with the largest oscillatory strength coincides with the lowest in energy, and thus, the final emission can be assumed to be due to this state only.

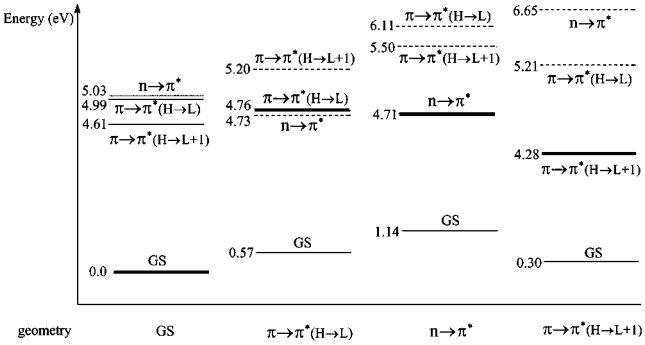

Figure 2. Solution energy level diagram for 9H Ade: all energies (in eV) are with respect to the ground state (GS) energy at its optimized geometry. Dotted lines refer to excited states in the presence of a "decoupled" solvent, normal lines refer to states in the presence of a nonequilibrium solvent, and bold lines refer to states in the presence of a fully equilibrated solvent.

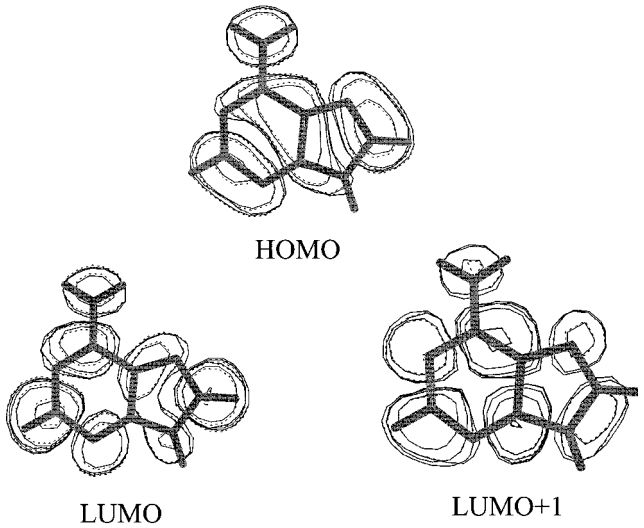

Figure 3. Molecular orbitals involved in the two $\pi \rightarrow \pi^*$ transitions of 9H Ade in water solution.

It is notable that for both Ade and 2AMP, the results computed for solvated systems are by far closer to experiments[26] than gas-phase analogues, showing once more the importance of a proper solvation model to have reliable computed−experimental comparisons.

3.4.1. Deactivation Mechanisms. To analyze possible deactivation mechanisms which operate on Ade but not on its isomer, 2AMP, in Figures 2 and 3, we report the energy level diagrams for 9H Ade in vacuo and in solution as a function of geometry. In particular, the geometries we have selected refer to ground state (and thus we have the absorption spectrum) and the $n \rightarrow \pi^*$ and $\pi \rightarrow \pi^*$ excited states, respectively; for the reasons reported above, in solution we have considered two different $\pi \rightarrow \pi^*$ excited states, corresponding to the states previously defined as HL and HL1. We stress that the data computed for the solvated system at the geometries optimized for an excited state are obtained with the solvent response equilibrated to the electronic state corresponding to the selected geometry, and thus, in each set, all the other excited states are computed with a "decoupled" solvent, indicating with "decoupled" a solvent which is equilibrated to a different state and thus seen as fixed. On the contrary, to have data coherent with the emission spectrum, we computed the ground-state values differently, namely, using a nonequilibrium scheme with a solvent not completely decoupled but instead partially relaxed according to the ground-state electronic charge distribution.

The two figures refer to 9H tautomer in vacuo and in solution, respectively.

Starting from the ground-state geometry, an important difference to note between gas-phase and solution results is the relative position of $n \rightarrow \pi^*$ excited state, which is shifted from the lowest state in gas phase to the third one in solution; this is easily explained in terms of a preferential stabilization of the more dipolar $\pi \rightarrow \pi^*$ excited states with respect to $n \rightarrow \pi^*$ in a polar solvent like water. The resulting effect is that the $n \rightarrow \pi^*$ state, which in gas phase is very close in energy to the lowest $\pi \rightarrow \pi^*$ state (i.e., to the HL1 state), becomes almost degenerate with the second $\pi \rightarrow \pi^*$ state (i.e., the HL state), indicating a very probable coupling between them. When the results obtained at the other geometries (corresponding to minima on the potential energy surfaces of each excited state) are added, the main feature to note in gas phase is that the $n \rightarrow \pi^*$ state remains the lowest one at all geometries, and we can suggest a probable avoided crossing between the two $\pi \rightarrow \pi^*$ states (which invert their relative positions passing from ground-state geometry to that corresponding to HL); at the $n \rightarrow \pi^*$ geometry, the HL1 state is very high in energy, and thus, it has not been reported in the diagram.

From these results, the most probable mechanism one can suggest for the isolated system is that the excited-state reached from the ground state upon absorption of one photon (the $\pi \rightarrow \pi^*$ HL state), by geometrically relaxing, is mixed with the other $\pi \rightarrow \pi^*$ state (the less probable HL1 state), with consequent population of both of them. However, this mixing is not sufficient to stabilize the states enough to shift them below the $n \rightarrow \pi^*$ state, which, vibronically interacting with them, can be populated with following quenching of the fluorescence.

In solution, the results indicate a more complex picture; the avoided crossing between HL1 and HL $\pi \rightarrow \pi^*$ states still remains, but in addition, the $n \rightarrow \pi^*$ state is no longer the lowest state at all geometries (in particular, the absolute minimum energy is that corresponding to the minimum of the HL1 state). As done for the gas phase, if we assume here that upon absorption the state which is mainly populated is the HL state, we can suggest that the final emission will be almost negligible due to the very probable shifting toward the $n \rightarrow \pi^*$ state, which will radiationlessly convert to the ground state. Clearly, this scheme is just one of the mechanisms which might be operative, and further analyses are worth being done.

Recent experimental observations on several alkylamine derivatives have shown that these systems give dual fluorescence; i.e., in addition to the normal weak short wavelength fluorescence, a long wavelength emission was observed. These findings seem to suggest that a twisted intramolecular charge transfer (TICT) could be operative also in Ade but this time as a deactivation mechanism. To check this model, we have studied the potential energy curves of the ground state and of the three excited states of Ade as a function of the dihedral angle between the amino group and the plane of the aromatic group. This analysis has been limited to the solvated 9H tautomer only, and the results are reported in Figure 4.

At each value of the dihedral angle, we have repeated the optimization of the geometry of the HL state at the CIS level: it is in fact this state which is mainly populated upon absorption. Also, we have assumed here that the solvent can completely equilibrate with the solute electronic state of interest during the geometry optimization. The resulting geometries are reported in the figure to have a more direct evaluation of the important geometrical changes along this coordinate (in particular, the out of plane motion of the amino group). Once the CIS optimized

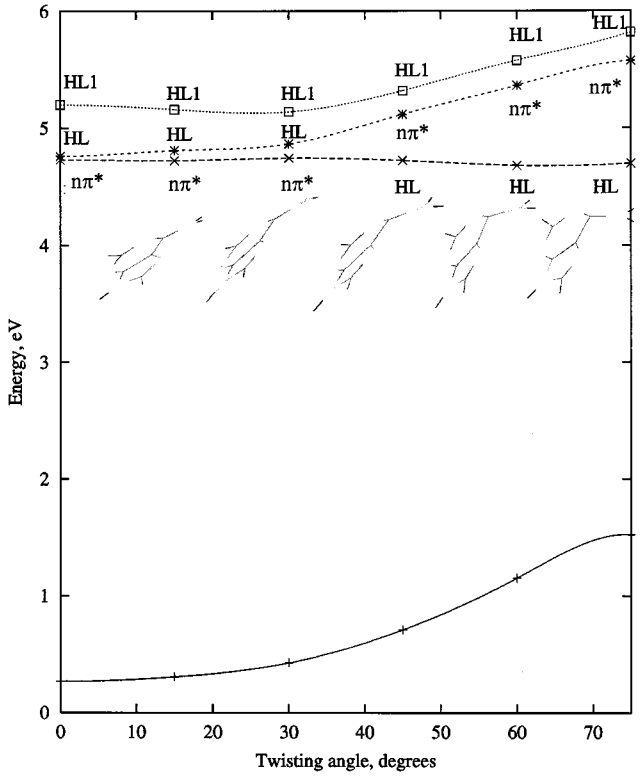

Figure 4. Ground and low-lying singlet excited states potential curves (energy relative to the minimum of the ground state) of 9H Ade in water solution as a function of the twisting angle. Energies are in eV and angles in degrees.

geometries are obtained, the corresponding electronic energies were computed at the CIPSI level in the presence of an equilibrium solvent. The CIPSI curves reported in Figure 4 show an avoided crossing between the two first excited states, indicated here with the generic S_1 and S_2 labels, due to their changing nature that cannot be univocally associated to the same transition along the coordinate.

From 0° to the avoided crossing, S_1 presents $n \rightarrow \pi^*$ character and S_2 HL, while after the crossing the respective character is reversed. The two states are very close up to the avoided crossing; therefore, a nonadiabatic transition from S_2 to S_1 should be likely in the range 0°−40°. Recalling that the curves have been optimized for the HL state, one could argue that S_1, once populated, should be stabilized due to both nuclear and solvent relaxation with following separation in the energy. However, in Figure 3, we have shown that the $n \rightarrow \pi^*$ optimum energy (i.e., at its optimized geometry and with an equilibrated solvent) is just 0.05 eV below the corresponding value obtained at the geometry and the solvent reaction field of the HL state; this should be sufficient proof that the almost flat curve reported in Figure 4 for S_1 before the avoided crossing is a valid description also for the relaxed state. In this scheme, if S_1were populated, a fast access to the HL portion of the curve would be very probable with following fluorescence decay. It is thus clear that the TICT mechanism alone cannot account for the extremely low fluorescence quantum yield of Ade (at least in water).

In water solution, a further possibility can be considered; this is related to the role of the second $\pi \rightarrow \pi^*$ state (the HL1). The relative position in the energy level diagram of the optimized excited states seems to suggest that the HL1, and not the HL, is the state which determines the fluorescence behavior of Ade (at least its 9H tautomer). In fact, at the HL1 geometry, we find that this state becomes the lowest state, with all the others well separated in energy (in particular, with $n \rightarrow \pi^*$ state well above the two $\pi \rightarrow \pi^*$states; see Figure 3). This large separation should prevent possible couplings between HL1 state and $n \rightarrow \pi^*$ contrary to what was found for the parallel HL state; however, HL1 has a small transition dipole moment (see Table 4), and thus, the fluorescence lifetime could still be large enough to observe a further radiationless decay to the ground state by vibronic couplings and/or solvent-induced quenching. On the contrary, if some emission can be observed, the corresponding computed emission energy agrees exactly with the low measured fluorescence (3.99 eV).

In this attempt to rationalize the possible mechanisms leading to the low fluorescent character of Ade, we have also to include a further possibility which has been extrapolated from experiments, namely, that the major part of the emission of Ade comes from the 7H tautomer. In the previous section, we have shown that from our calculations the emission energy of 7 Ade was in slightly better agreement with experiments than 9H tautomer (4.14 eV vs 4.18 eV with respect to 3.99 eV) if it was assumed that only the $\pi \rightarrow \pi^*$ HL state contributes to the fluorescence of 9H Ade. Here we can add that for 7 Ade the analysis is far simpler; as no interactions between HL and HL1 $\pi \rightarrow \pi^*$ states have to be introduced (HL is in fact both the most probable and the lowest excited state), possible mechanisms for quenching of the fluorescence reduce to coupling between the HL $\pi \rightarrow \pi^*$ and the $n \rightarrow \pi^*$ states, following radiationless vibrational transition to the ground state.

As clearly shown by experiments, the situation is completely different for 2AMP, for which an high fluoresce is observed in polar solvent. This is completely confirmed by our calculations in water solution; contrary to what was found for Ade, in fact, for 2AMP, the $\pi \rightarrow \pi^*$ excited state reached by absorption (i.e., that with the largest oscillatory strength) is always well separated from the all others states (e.g., $n \rightarrow \pi^*$ and the other $\pi \rightarrow \pi^*$), and consequently, the resulting fluorescence is strong and completely due to a single emitting state. For 2AMP, we have not reported the corresponding energy diagrams at the various geometries, as the absorption and emission energies by themselves exhaustively prove the agreement of computational results and the experimental evidence.

4. Summary

Extensive calculations of the ground and the lowest single excited states of adenine have been carried out using different quantum mechanical levels. In all calculations, we have included the effects of the solvent either assuming a complete equilibrium with the solute nuclear and electronic charge distribution or introducing a partial nonequilibrium when fast transition processes are considered. Solvent effects on both nuclear and electronic relaxation of the ground and the excited states have been described in terms of a continuum model (the IEF), taking into account electrostatic and repulsive solute−solvent interactions and exploiting an accurate molecular cavity modeled on the real structure of the molecular solute. To have a more complete description of the photophysical properties of adenine, we have considered both the N(7)H and N(9)H tautomers as well as adenine's highly fluorescent isomer, 2-aminopurine.

Absorption and emission spectra in gas phase and in water solution have been simulated at the CIPSI (and TDDFT for absorption) level of calculation and compared (in the case of water solution) with available experimental data; the very good agreement obtained for both confirms the accuracy of our approach (CIS geometries + CIPSI electronic descriptions, both coupled with the IEF solvation model), as already shown in a previous application on the photophysics of dimethyl aminobenzonitrile (DMABN).[35]

This agreement has then allowed us to apply the approach to the analysis of different possible deactivation mechanisms acting on solvated Ade but not on its isomer 2AMP. The analysis has been mainly focused on solvated 9H tautomer, being the major component in water solution, and two different mechanisms have been considered: the proximity and the intramolecular twisting effect.

For the proximity effect, our calculations showed that a state crossing occurs during the excited-state nuclear relaxation following a shift of the $n \rightarrow \pi^*$ state below the $\pi \rightarrow \pi^*$ state reached upon excitation. Following this scheme, a rapid radiationless conversion from the $n \rightarrow \pi^*$ state to the ground state by vibrational deactivation seems very probable. On the contrary, this cannot happen for 2AMP for which the lowest state maintains a $\pi \rightarrow \pi^*$ character also after nuclear relaxation: in particular, the separation between $\pi \rightarrow \pi^*$ and $n \rightarrow \pi^*$ states of 2AMP is increased in solution according to the experimental evidence of an increased quantum yield with increasing solvent polarity.

Passing to the effect of an intramolecular twisting of the amino group in the $\pi \rightarrow \pi^*$ state reached upon excitation, the computed curves showed that such mechanism alone cannot account for the extremely low fluorescence quantum yield of Ade (at least in water). In fact, for small twisting angles, the two lowest excited states are very close, and they present $n \rightarrow \pi^*$ and $\pi \rightarrow \pi^*$ character, respectively, but after the avoided crossing, the respective character is reversed, and the corresponding curves begin to diverge. In this framework, a transition from $\pi \rightarrow \pi^*$ to $n \rightarrow \pi^*$ becomes very probable. However, even if the $n \rightarrow \pi^*$ state were populated, a fast access to the $\pi \rightarrow \pi^*$ portion of the curve would be likely to happen with following fluorescent decay in contrast with the experimentally evidence.

For solvated Ade,however, a further mechanism related to the second $\pi \rightarrow \pi^*$ state (the HL1) was also considered. In fact, at HL1 optimized geometry, all the excited states are well separated in energy, with $n \rightarrow \pi^*$ state well above the two $\pi \rightarrow \pi^*$ states. This separation in energy should disfavor any coupling; however, the HL1 state has a small transition dipole moment, and thus, the fluorescence lifetime could be large enough to observe a further decay directly to the ground state by vibronic couplings and/or solvent-induced quenching. On the contrary, if we assume that HL1 has time to emit, the corresponding computed emission energy was found in exact agreement with the measured fluorescence (3.99 eV). Both these aspects seem to suggest that the HL1, and not the HL, is the state which determines the fluorescence behavior of 9H tautomer of Ade.

All the hypotheses we have analyzed cannot give the definitive answer to the fundamental question on the mechanism developed by nature to avoid damaging photochemistry in the nucleic acid bases (here the adenine); however, our study can be seen as one of the first attempt to get accurate theoretical data on complex molecular systems in the environment in which they exist in nature. Much more work has still to be done, especially in order to take into proper account the dynamical aspects of excited-state relaxations also including the dynamics of the solvent molecules; but first, accurate ab initio studies accurately reproducing absorption and emission spectra as well as excited-state nuclear and electronic structures are required. Our study represents an example of this first phase, but further studies belonging to the second phase are already in progress.

References and Notes

(1) Callis, P. R. *Annu. Rev. Phys. Chem.* **1983**, *34*, 329.

(2) Holmen, A.; Norden, B.; Albinsson, B. *J. Am. Chem. Soc.* **1997**, *119*, 3114.

(3) (a) Miertus, S.; Scrocco, E.; Tomasi, J. *Chem. Phys.* **1981**, *55*, 117. (b) Cammi R.; Tomasi, J. *J. Comput. Chem.* **1995**, *16*, 1449.

(4) (a) Cancès, E.; Mennucci, B. *J. Math. Chem.* **1998**, *23*, 309. (b) Cancès, E.; Mennucci, B.; Tomasi, J. *J. Chem. Phys.* **1997**, *107*, 3032. (c) Mennucci, B.; Cancès, E.; Tomasi, J. *J. Phys. Chem. B* **1997**, *101*, 10506.

(5) Frisch, M. J.; Trucks, G. W.; Schlegel, H. B.; Scuseria, G. E.; Robb, M. A.; Cheeseman, J. R.; Zakrzewski, V. G.; Montgomery, J. A., Jr.; Stratmann, R. E.; Burant, J. C.; Dapprich, S.; Millam, J. M.; Daniels, A. D.; Kudin, K. N.; Strain, M. C.; Farkas, O.; Tomasi, J.; Barone, V.; Cossi, M.; Cammi, R.; Mennucci, B.; Pomelli, C.; Adamo, C.; Clifford, C. S.; Ochterski, J.; Petersson, G. A.; Ayala, P. Y.; Cui, Q.; Morokuma, K.; Malick, D. K.; Rabuck, A. D.; Raghavachari, K.; Foresman, J. B.; Cioslowski, J.; Ortiz, J. V.; Stefanov, B. B.; Liu, G.; Liashenko, C. A.; Piskorz, P.; Komaromi, I.; Gomperts, R.; Martin, R. L.; Fox, D. J.; Keith, T.; Al-Laham, M. A.; Peng, C. Y.; Nanayakkara, A.; Gonzalez, C.; Challacombe, M.; Gill, P. M. W.; Johnson, B.; Chen, W.; Wong, M. W.; Andres, J. L.; Head-Gordon, M.; Replogle, E. S.; Pople J. A. *Gaussian 99, Development Version*; Gaussian: Pittsburgh, PA, 1999.

(6) (a) Becke, A. *J. Chem. Phys.* **1993**, *98*, 5648. (b) Stephens, P. J.; Devlin, F. J.; Chabalowski, C. F.; Frisch, M. J. *J. Phys. Chem.* **1994**, *98*, 11623.

(7) Woon, D. E.; Dunning, T. H., Jr. *J. Chem. Phys.* **1993**, *98*, 1358.

(8) (a) Cancès, E.; Mennucci, B. *J. Chem. Phys.* **1998**, *109*, 249. (b) Cancès, E.; Mennucci, B.; Tomasi, J. *J. Chem. Phys.* **1998**, *109*, 260.

(9) Cammi, R.; Mennucci, B.; Tomasi, J. *J. Phys. Chem. A* **2000**, *104*, 5631.

(10) (a) Huron, B.; Malrieu, J.-P.; Rancurel, P. *J. Chem. Phys.* **1973**, *58*, 5745. (b) Evangelisti, S.; Daudey, J.; Malrieu, J.-P. *Chem. Phys.* **1983**, *75*, 91. (c) Spiegelmann, F.; Malrieu, J.-P. *J. Phys. B* **1984**, *17*, 1235. (d) Cimiraglia, R. *J. Chem. Phys.* **1985**, *83*, 1746. (e) Cimiraglia, R.; Persico, M. *J. Comput. Chem.* **1987**, *8*, 39.

(11) Angeli, C.; Persico, M. *Theor. Chem. Acc.* **1997**, *98*, 117.

(12) Angeli, C.; Cimiraglia, R.; Persico, M.; Toniolo, A. *Theor. Chem. Acc.* **1997**, *98*, 57.

(13) Mennucci, B.; Toniolo, A.; Cappelli, C. *J. Chem. Phys.* **1999**, *110*, 6858.

(14) Schmidt, M. W.; Baldridge, K. K.; Boatz, J. A.; Elbert, S. T.; Gordon, M. S.; Jensen, J. H.; Koseki, S.; Matsunaga, N.; Nguyen, K. A.; Su, S. J.; Windus, T. L.; Dupuis, M.; Montgomery, J. A. *J. Comput. Chem.* **1993**, *14*, 1347.

(15) Tomasi, J.; Persico, M. *Chem. Rev.* **1994**, *94*, 2027.

(16) Amovilli, C.; Mennucci, B. *J. Phys. Chem. B* **1997**, *101*, 1051.

(17) Dreyfus, M.; Dodin, G.; Bensaude, O.; Dubois, J. E. *J. Am. Chem. Soc.* **1975**, *97*, 2389.

(18) Brown, R. D.; Godfrey, P. D.; Mcnaugthon, D.; Pierlot, A. P. *Chem. Phys. Lett.*, **1989**, *156*, 61.

(19) Wilson, R. W.; Callis, P. R. *Photochem. Photobiol*. **1980**, *31*, 323.

(20) De Voe, H.; Tinoco, I., Jr. *J. Mol. Biol.* **1962**, *4*, 500.

(21) McMullan, R. K.; Benci, P.; Craven, B. M. *Acta Crystallogr., B* **1980**, *36*, 1424.

(22) Harnden, M. R.; Jarvest, R. L.; Slawin, A. M. Z.; Williams, D. J. *Nucleosides Nucleotides* **1990**, *9*, 499.

(23) Holmen, A.; Broo, A.; Albinsson, B.; Norden, B. *J. Am. Chem. Soc.* **1997**, *119*, 12240.

(24) Broo, A.; Holmen, A. *Chem. Phys.* **1996**, *211*, 147.

(25) Jean, J. M.; Hall, K. B. *J. Phys. Chem. A* **2000**, *104*, 1937.

(26) Broo, A. *J. Phys. Chem. A* **1998**, *102*, 526.

(27) Eisenstein, M. *Acta Crystallogr.* **1988**, *B44*, 412.

(28) Holmen, A.; Broo, A. *Int. J. Quantum Chem.* **1995**, *QBS22*, 113.

(29) Clark, L. B.; Peschel, G. G.; Tinoco, I. *J. Phys. Chem.* **1965**, *69*, 3615.

(30) Stewart, R. F.; Davidson, J. *J. Chem. Phys.* **1963**, *39*, 255.

(31) Clark, L. B. *J. Phys. Chem.* **1990**, *94*, 2873.

(32) Clark, L. B. *J. Phys. Chem.* **1995**, *99*, 3366.

(33) Fülscher, M.; Serrano-Andres, L.; Roos, B. O. *J. Am. Chem. Soc.* **1997**, *119*, 6168.

(34) Rachofsky, E. L.; Ross J. B. A.; Krauss, M.; Osman, R. *J. Phys. Chem. A* **2000**, *104*.

(35) Mennucci, B.; Toniolo, A.; Tomasi, J. *J. Am. Chem. Soc.* **2000**, *122*, 10621.